FORMING ANALYSES OF DP600 STEEL USING DIFFERENT BLANK-HOLDER PRESSURES

Luiz Maurício Valente Tigrinho, luiz.tigrinho@ifpr.edu.br
Departamento de Mecânica - Instituto Federal de Educação, Ciência e Tecnologia do Paraná – Campus Curitiba
CEP 80.230-150 – Curitiba – Paraná – Brasil.

Ravilson Antonio Chemin Filho, ravilson@ufpr.br
Rosalvo da Cunha Barreto Neto, rosalvo.barreto@gmail.com
Sérgio Fernando Lajarin, espanhol@ufpr.br
Paulo Victor Prestes Marcondes, marcondes@ufpr.br
Departamento de Engenharia Mecânica - Centro Politécnico – Universidade Federal do Paraná - Caixa Postal 19011
CEP 81531-990 – Curitiba – Paraná – Brasil.

Abstract: *Changes are often required during the try-and-error procedure of drawing tools. These changes may range from adjustments in die and punch designs and other factors like blank-holder pressure. All these actions, however, require time and money, thus raising the need for improved initial evaluations of thin sheet metal. Increasing interest is therefore being estabilished in the development of laboratory tests that allow stamping manufacturers to become more familiar with the stamping ability of the thin sheet metal they use, thereby ensuring, at least in part, that the pieces manufactured are stamped without major problems. The sheet metal forming is highlighted among the manufacturing processes, especially in the auto industry, which has had a growing concern about the safety of vehicles and emissions from them. Cars must be light and safe and, therefore, require the use of thin and resistant plates. As a result, the application of new materials such as AHSS (Advanced High Strength Steel), for example, DP steels (Dual Phase) has increased. In this work, three different blank-holder pressures, 10, 14 e 22 MPa, were used in addition to the traditional Nakazima drawing test tool. Thus, an evaluation was made of how the different blank-holder pressures affected the forming limit of DP600 steel. The results obtained were investigated by the diagram force vs punch displacement, forming limit diagram and fracture analyses. The results obtained were investigated by the diagram force vs punch displacement, forming limit diagram and fracture analysis. The results were compared experimenting with analysis by finite element methods where the computational limitations have been observed to predict the time of fracture.*

Keywords*: Forming, AHSS, DP600 steel, blank-holder pressure.*

1. INTRODUCTION

The automobile industry is one of the largest markets for high-strength steels and a major driving force for the development of new materials and technologies. In recent decades, the increased competition and growing demand for safer, economical and less polluting cars, demanded of automakers, steelmakers and the scientific community investments in search of new steels. The result of these studies was the significant increase in the use of advanced high strength steels in automobiles.

The ongoing technological evolution of consumer goods and the need to develop an adequate infrastructure to meet the vital needs of humanity has imposed the development of relatively inexpensive materials whose performance met the mechanical, chemical and physical requirements needed for many applications. The flat steel products have virtually universal application, thanks to the ability they have to assume the most varied profiles of properties through the careful choice of alloys and the application of specific thermal or thermomechanical treatments.

To reduce costs and optimize the process, an understanding of the formability of sheet metal is essential to produce quality stamped parts. Process planners and tool designers must define the formability level required for each part, so that they can be sure to know the deformation level of the material they use.

This present work aim is to determine the mechanical properties and analyze the fracture of DP600 steel sheets after stamping tests. It is necessary also to analyze the metallurgical behavior of materials, investigating properties that affect the behavior of material during metal forming, mainly during the propagation of cracks.

1.1. Advanced High Strength Steel (AHSS)

The design of new alloys is always associated with the demands and the continuous challenges of the steel market. When you combine a good alloy design with an appropriate thermomechanical processing, numerous combinations of properties can be obtained such as high resistance associated with the ductility, toughness and formability. The coexistence of these mechanical properties is only possible due to the presence of different microstructural constituents, according to Bhadeshia (2001), Bleck (2005) and Gorni (2008).

The issue of the development of new alloys for use in the automotive industry is so prevalent that in the past 20 years, several projects are underway, involving the scientific community and major steel manufacturers in the world. The main objective of this sector has been to offer increasingly innovative materials, production methods and assembly techniques that are most appropriate to their needs, focusing on achieving an ever higher level of safety and decrease vehicle weight, according to Andrade et al. (2002), De Cooman (2004) and Grajcar (2005).

Could be highlighted the project entitled Ultra Light Steel Auto Body - ULSAB under the leadership of Porsche Engineering that has a partnership of 35 steel companies from 18 countries. One of the benefits from this major initiative was the introduction of high strength steels - HSS (High Strength Steel) in the automobiles' structures , mainlly among those the Bake-Hardening Steels - BH Steel and High Strength Low Alloy - HSLA (High Strength Low Alloy). Completed in 1998, the project was satisfactory rated in relation to the desired goals, especially in regard to safety and reduction in fuel consumption according to Andrade et al. (2000).

Following the project ULSAB, the new program ULSAB-AVC (Advanced Vehicle Concepts) proposes the application of new HSLA steels, the so-called "high-resistance last generation steels" - AHSS (Advanced High Strength Steel), among those can be nominated the Dual Phase steels – DP; the Deformation Induced Plasticity steels – TRIP; the Complex Phase steels- CP and the Martensitic Steels - MART. The AHSS steels are multiphase materials that may contain into the microstructure: Ferrite, martensite, bainite, and / or retained austenite, depending on the alloying elements and processing used, Andrade et al. (2000).

1.2. Dual Phase (DP) Steel

One of the resources available to maximize both the ductility and mechanical strength of steels is the use of more complex microstructures than ferritic or ferritic-pearlitic normally present in the common low-carbon alloys. This approach is based on more complex interactions between the various constituents of the microstructure, which also must have significant variations in hardness among themselves. In the late 1970s was discovered the first development in this direction, the so-called biphase steel (dual phase), as its name implies, has a microstructure consisting of a matrix with 80 to 85% of polygonal soft ferrite and 15 to 20 % of hard martensite, Rashid (1977).

Hornbogen (1980) defined the two-phase microstructure as a merger of the three basic morphologies of the micro-structure with two phases: duplex, dispersion and network. Therefore, the two-phase microstructure has the characteristics peculiar to each topological type of morphology. As occured with the duplex microstructure, in two-phase microstrucure, quantities of grains per volume of both phases are equal, therefore the ratios between the volumes of grains between the two phases and their volume fractions must be equal. From the microstructure suffering dispersion, results that at the biphasic, the second hard phase must be completely isolated by the soft matrix phase, ensuring the ductility and formability of the material. Finally, just as the network microstructure in the biphasic, the second phase is located exclusively in the grain boundaries of the matrix phase, Gorni (1995).

During the production of dual phase steels, both by the hot sheet rolling and by continuous annealing, the ferrite matrix is formed first, thereby enriching the remaining austenite with carbon and other alloying elements. This, in turn, earns enough hardenability to transform to martensite later, under much lower temperatures. This delayed processing of martensite induces compressive residual stresses at the ferritic matrix, which facilitate the process flow and thereby reduce the value of the yield stress and suppress the occurrence of a plateau. A slow cooling after the formation of martensite can provide reduction of the fragility of the newly formed martensite by tempering effects. During plastic deformation the flow of soft ferrite matrix through the islands of hard martensite hardens the material significantly, helping to increase their strength.

In ferritic steels with low carbon and high formability, the correlations between microstructure and mechanical properties are relatively simple, since the microstructure is characterized only by the size and shape of their grain, as well as their crystallographic texture. The situation is more complex regarding dual phase steels, since the characterization of its microstructure is more difficult, involving parameters such as grain size of both phases, the ratio between their hardness, the mean free path of ferrite and the degree of contiguity between the two phases, Gorni (1995).

2. EXPERIMENTAL PROCEDURE

The aim of this study is to ascertain the mechanical properties and fracture analysis of DP600 steel sheets after stamping tests. The steel sheet used in the tests has a thickness of 2.0 mm and was supplied by Usiminas.

It was required a preliminary analysis of the material to be used in the tests. This analysis begun with a metallographic test to verify the metallographic texture of the material and identify the present phases at the steel. After that it was carried out a chemical analysis to verify the chemical composition of the sheets used at the tests.

Following that, tensile tests were performed to disclose the mechanical properties and the parameters of formability of the material. Also it was performed the Nakazima (1968) method of stamping with hemispherical punch (Fig. 1a), to obtain the forming limit curve of the sheet metal.

Finally, in order to characterize the type of fracture occurred at the DP600 steel, after the tests with different stamping pressure on blank-holder, tests were conducted with the SEM (Scanning Electron Microscope).

2.1 FE-Model

The simulation of the Nakazima's test was performed with the commercial FEM software package ABAQUS/Explicit using a tri-dimensional model. The sheet has been meshed with shell elements with four knots and six degrees of freedom (S4R) with 7 integration points at the thickness (ABAQUS, 2009). In the stretching region of the sheet was used a mesh with with elements of 1 mm per side. The punch, die and blank-holder have been considered as analytic rigid surfaces. The contact between the sheet and the tools was described by the Coulomb friction model with a friction coefficient of 0.1. The loads at the blank-holder were changed as experimental values: 10, 14 and 22 MPa. The sheet material used was the 2 mm DP600 steel.

Due to the problem is symmetrical, only one quarter of the geometry of the plate was modeled (Fig. 1c). Were set out three steps in the simulation model, in the first, the blank-holder detaches slowly touching on the plate, at the the second, the blank-holder applies the load on the plate, and, at the third, the punch moves into the die deforming the plate.

The material model used was the Von Mises isotropic hardening (assumes the material properties similar in all directions). The determination of the damage initiation criteria were made via the ductile damage initiation criteria that predict the damage initiation due to nucleation, growing and coalescence of voids in ductile materials. The details of the definition of the criteria are detailed in Lajarin et al. (2010).

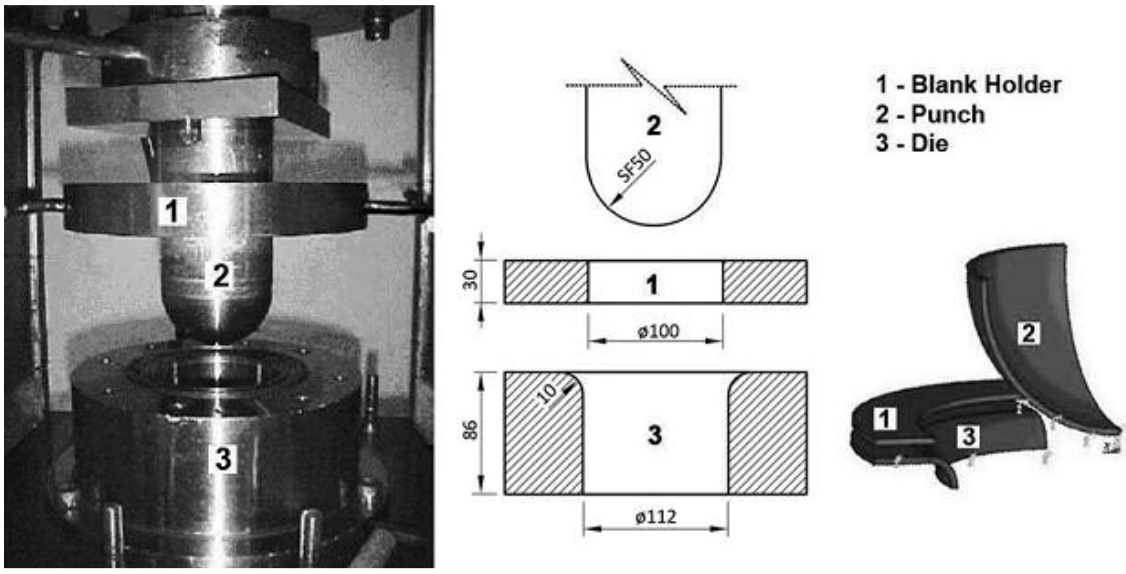

(a) (b) (c)

Figure 1. Tooling proposed by Nakazima: (a) assembled tool, (b) tool dimensions in mm and (c) FE model.

3. RESULTS AND DISCUSSION

3.1. Chemical composition

Aiming to know the chemical composition of the study material, it was performed a chemical analysis test with an optical emission spectrometer. Chemical analysis of the material allowed the determination of the actual composition of the sample provided by the manufacturer of steel for the tests. The Table 1 shows the chemical composition in mass of the DP600 steel.

Table 1. Chemical composition (%) of the test results of chemical analysis of DP600 steel.

Chemical composition of DP600 steel (mass %) - Supplied by manufacturer												
C	Si	Mn	P	S	Al	Cr	Nb	V	Ti	Ni	Mo	N
0,07	0,01	1,66	0,019	0,005	0,043	0,03	0,015	<0,005	<0,005	0,02	0,16	0,0058
Chemical composition of DP600 steel (mass%) - Lab test												
C	Si	Mn	P	S	Al	Cr	Nb	Zr	Ti	Ni	Mo	Cu
0,086	0,053	1,739	0,027	0,027	0,031	0,048	0,028	0,006	0,004	0,029	0,226	0,094

Comparing the data provided by the steel manufacturer with a lab test, it is possible to state that this is really the DP600 steel, by the chemical similarity between the results with a discrepancy between the results in the amount of sulfur (S).

This chemical composition presented by the material gives a certain level of formability of the DP600 steel without loss of mechanical strength.

3.2. Metallography

Through metallographic tests it was possible to determine the grain morphology and to identify the present phases in the steel DP600. Figure 2 shows the micrographs with a magnification of 800x and 3500x.

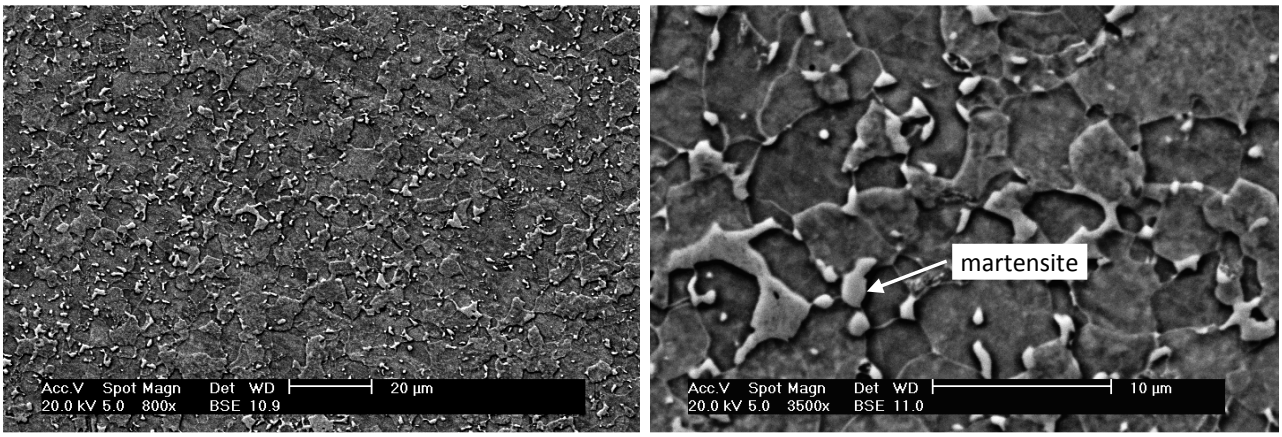

(a) 800x (b)3500x

Figure 2. Micrograph of the DP600 steel with islands of martensite in a ferritic matrix.

Figure 2 illustrates the microstructure of steel DP600, containing islands of martensite (light portion) dispersed in the ferrite matrix (dark portion). The soft ferrite phase is usually continues, giving these steels an excellent ductility. When these steels deform, the deformation is concentrated at the lower resistance phase (ferrite) around the islands of martensite, providing a high strain hardening rate for these steels.

3.3 Mechanical properties

Tensile tests, performed with the specimens forming angles of 0, 45 and 90 ° to the rolling direction, provided information on mechanical properties such as tensile strength (UTS), yield stress (YS) , elongation (El.), anisotropy factor (Lankford "R") and strain hardening coefficient ("n" exponent) of the material. These two last parameters are needed to characterize the material formability.

Table 2 shows the results on the mechanical properties of the material obtained through the tensile tests, compared to the figures provided by the manufacturer of the DP600 steel.

Table 2. Comparison of the YS, UTS and El. mechanical properties of the DP600 steel, supplied by the manufacturer of steel and obtained from tensile tests.

Mechanical properties of the DP600 steel			
Properties	YS (MPa)	UTS (MPa)	*El.* (%)
Supplied by the manufacturer	385	621	23,9
Tensile tests	410	640	28,5

The results shown in Table 2 stated that both the UTS values as the YS and El., obtained by tensile tests, fit perfectly within the range preset by the steel manufacturer, without exceeding or even approaching the range determined limit. This ensures that, in terms of mechanical properties, the steel sample to be used in subsequent testing shows no restriction that may influence the results of laboratory after.

The parameters R en formability of the sheet, obtained by tensile tests are presented in Table 3. The values were obtained by performing a minimum of three trials for each direction of the specimen, then, an average was calculated for each direction, as provided by the NBR 8164. Table 3 also shows the anisotropy average value ($\bar{R}$) and the planar anisotropy (ΔR).

Table 3. Formability parameters R, n, $\bar{R}$ and ΔR, of the DP600 steel supplied by the manufacturer and obtained by tensile tests.

Formability parameters of the DP600 steel									
Parameters	$\bar{R}$	$R_{0°}$	$R_{45°}$	$R_{90°}$	ΔR	$n_{average}$	$n_{0°}$	$n_{45°}$	$n_{90°}$
Manufacturer	0,84	0,70	1,06	0,70	X	0,18	0,17	0,19	0,17
Tensile Tests	0,9356	0.6739	1,0354	0,9977	0,1996	0,1880	0,1892	0,1931	0,1818

The results of Table 3 reinforce that the DP600 steel is a material intended for operations that require a certain stamping degree, since the R factor and mainly the n coefficient values were high enough (the value ΔR = 0,1996 is extremely low, in disagreement with the other values found) near or above 1.0 for R and around 0.2 to *n*, in such mesure to to warrant this feature of the material. An important factor to note is the variation of the results of the R factor for each of three directions (0º, 45º and 90º), represented by $R_{0°}$, $R_{45°}$ and $R_{90°}$. In this case, the highest value of R was reached for the direction of 45 and then 90 degrees, around 1.03 and 1.00 respectively, implying that the material exhibits better formability in these directions, ie, shows a tendency to deform more efficiently in relation to efforts to rolling direction of the plate, reaching a higher deformation level without disruption at these directions. For the direction of 0 °, the value of R had the lowest value being in the range of 0.67. Compared with the values provided by the steel manufacturer, the only value that showed a significant difference was in the direction of 90 °, which showed a value close to 1.00 according to the test results, while the manufacturer provided a value of 0.70.

The hardening coefficient resulting from the tests was approximately 0.19 for each of the three directions in which the material was tested, represented by $n_{0°}$, $n_{45°}$ and $n_{90°}$ to the 0º, 45º and 90º respectively. From this Fig. 3 it can be said that the DP600 has a good formability. Like the R factor, the higher the value of the strain hardening coefficient *n*, the better the formability of the material, Kumar (2002). The result obtained for the exponent *n* in the tests shows that the material under study tends to be a high plastic instability limit, which gives good formability stretch, since the higher the instability threshold of the material, the material, when subjected to the stamping process, tends to distribute the deformation to the neighboring regions of the more deformed place, resulting in a more homogeneous thinning of the sheet. This avoids an occurrence of a thickness reduction in a localized portion of the material, which leads to the sheet rupture. Figure 3 shows the Stress-Strain graph of the DP600 steel obtained from the tensile test and make a comparison with other literature results.

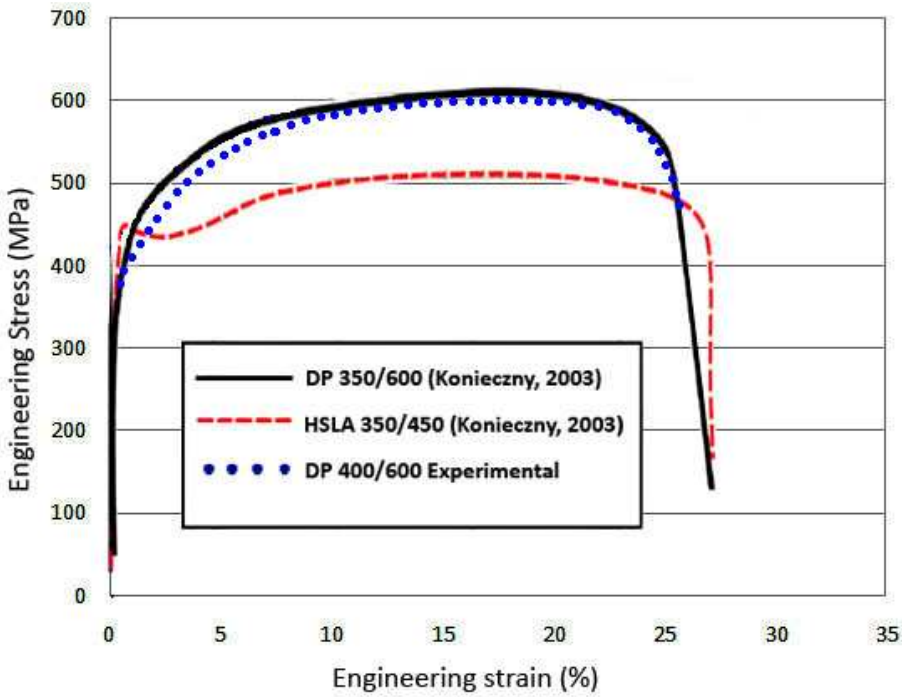

Figure 3. DP 400/600 steel stress vs. strain graph compared to the literature.

As can be seen in Fig. 3, the DP steel exhibits an initially higher hardening rate , larger UTS and smaller YS / TS than the HSLA. YS / TS is the ratio between the values of Yield Strength (YS) and Tensile Strength (TS). The steel tested showed higher elongation and higher hardening rate than the results of the literature. Konieczny (2003) mentions that the hardening rate combined with the its excellent elongation, gives the DP steel greater UTS (Ultimate Tensile Strength) than conventional steels of similar yield strength.

Analyzing the Fig. 3, there is a lack of a defined yield point at the end of the elastic region for the DP600 steel. This is an important information for stamping operations, since in this manufacturing process, this point could lead to defects in the final product, such as Lüders lines, according to Smith (1996), when the strain at some points reach a part of the plastic deformation but near the elastic region, causing this failure. This defect may still occur if the material is aged, which would be evidenced by rise in the position of yield point at the curve.

DP steels exhibit an excellent combination of high strength and deformation capacity, a result of its microstructure with a great capacity of strain hardening. The high strain hardening capacity of these steels ensures an improved absorption capacity of impact and fatigue resistance. All these features make the DP steels an interesting option for structural components and safety features in cars such as the cross bars of the door, the stringers, the A and B pillars, the door-frame sill, the arch roof, the bumper, among others (ACELORMITTAL, 2009).

3.4. Stamping

Assays were performed according to the Nakazima stamping method, without punch lubrication, in order to determine the Forming Limit Diagram (FLD) of the material by taking 8 samples (the dimensions of blanks ranged from 25x200mm to 200x200mm), the same amount used in previous work by Chemin Filho (2004) and Tigrinho (2008). Figure 4 shows the FLD obtained for the DP600 steel e compares with the FLD of the Mild Steel 170/300, 350/450 HSLA and DP 350/600 steels with a 1.2 mm thickness determined experimentally by Konieczny (2003).

The tests showed a FLD with a high degree of strain for the conditions of deep drawing, the left side of the curve (second quadrant), where the major strain (ε_1) reached 0.59 while the minor strain (ε_2) was 0.43. The plain strain, reached a major strain of 0.33 and the minor strain was zero. In contrast, for the right side of the curve, which represents the stretch condition, the maximum strain reached ε_1 was 0.41 and ε_2 was 0.23, ie, not as high. This fact showed a difficult feature of this type of test, which is, to achieve a comprehensive profile of the FLD to the stretch condition, allowing only small levels of strain ε_2.

It was evidenced the dependence of the lubrication at the deformation modes. In the deep drawing and the plain strain, the FLD had higher levels of strain (ε_1= 0.59, ε_2 = 0.43 and ε_1 = 0.33, ε_2 = 0, respectively), thereby demonstrating that these deformation modes not tend to be dependent on the lubrication, according to Keeler (2000).

At the deformation mode by stretching, the FLD was not fully represented, with low levels of deformation, ε_1=0,41 and mainly, ε_2=0,23, which demonstrates the dependence of this deformation mode with the lubrication, so that it has a reduced friction at the interface punch – metal sheet, and consequently higher levels of strain ε_2. The lubrication of the punch has no significative influence on deep drawing, whereas in the stretch, the punch should be well lubricated, so that the FLD can be extended to a higher level of deformation in the stretch, as reported by Keeler (1968) and Tigrinho (2005).

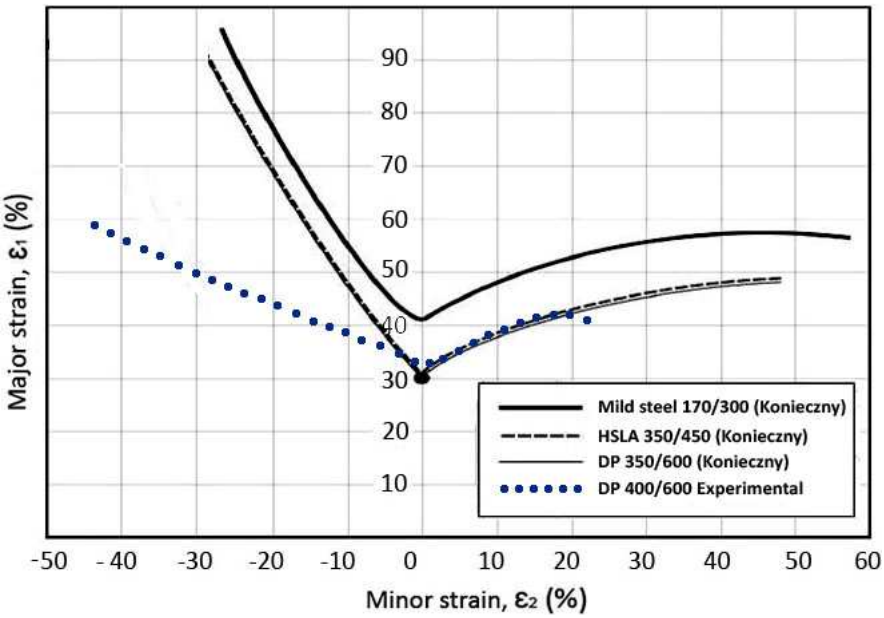

Figure 4. Forming Limit Diagram DP600 steel, obtained by the stamping test proposed by Nakazima compared with results obtained by Konieczny (2003).

The three curves obtitained by Konieczny (2003) showed approximately the same profile. Whereas the DP and HSLA steels have approximately the same value of *n*, the similar FLDs is expected. The Mild Steel has a higher curve due to the significantly greater value of *n* (WORLDAUTOSTEEL, 2009).

In comparison with the experimental results obtained in this work by the Nakazima testing it can be observed that the FLDs of the DP600 steels have a similarity only in the plain strain with ε_1=0.33 and ε_1=0.30. In other deformation modes, drawing and stretching, a comparison cannot be made, hence the curves showed a considerable discrepancy.

After determined the steel FLD, tests were done by stamping with the same hemispherical punch without lubrication and with 200x200mm samples, but now varying the pressure on the blank-holder. There were used 3 pressures: 10, 14 and 22 MPa, and stated the diagram of the punch displacement versus stamping force. In Figure 5 is showed the results of practical experiments and computer simulation. It can be observed in both cases that for a lower pressure at the blank-holder, the punch reached a greater stamping, thus requiring a greater forming force. In the experimental results of stamping forces reached 8x105, 9x105 and 10x105 N for the blank-holder pressures of 10, 14 and 22 MPa, respectively. The force values recorded in the simulation were close to the experimental results, but showed little variation of 8x105 N among the three blank-holder pressures. Furthermore, the simulation results were not accurate to predict the onset of the crack. As can be seen in Fig.5 for the drop in force curves indicate the onset of the crack, in the case of practical experiments cracks occurred after 40 mm (22 MPa), 48 mm (14 MPa) and 54 mm (10 MPa), while the simulation results indicated the occurrence of cracks after 50 mm (22 MPa), 54 mm (14 MPa) and 55 mm (10 MPa).

The difficulty in predicting the onset of the cracks under different conditions of blank-holder pressure is credited due to metallographic characteristics of the dual phase steel. Because it has two phases with distinct behavior, the interaction of these two phases is not sufficiently described by the constitutive equations of the material in the simulation package.

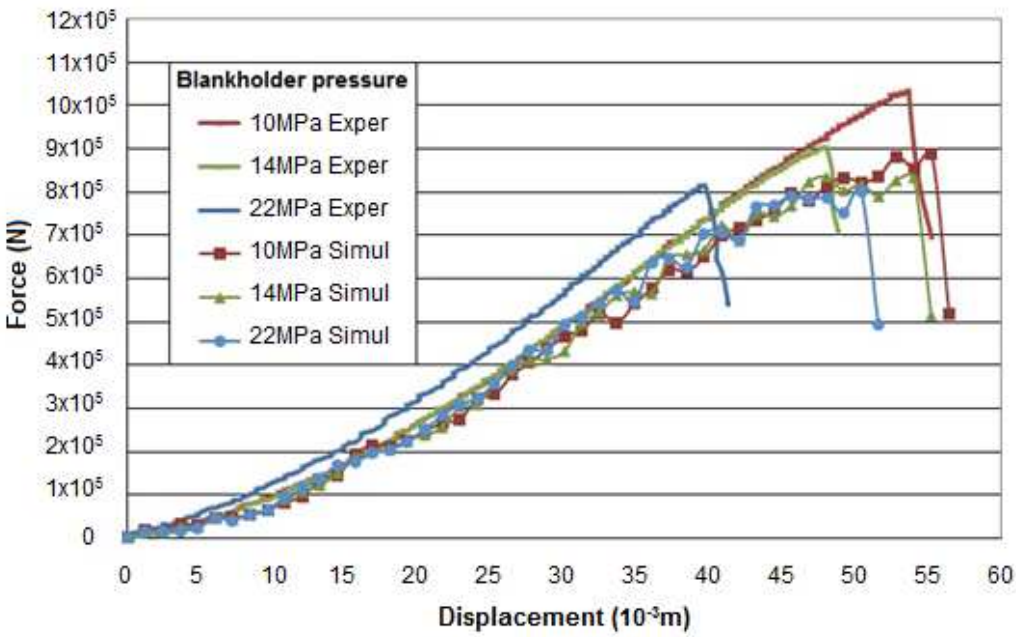

Figure 5. Experimental and simulation displacement of the punch vs. stamping force by varying the pressure at the blank-holder.

In the Fig. 6 is possible to notice the fracture place in the 200x200mm samples stamped without lubrication with hemispherical punch.

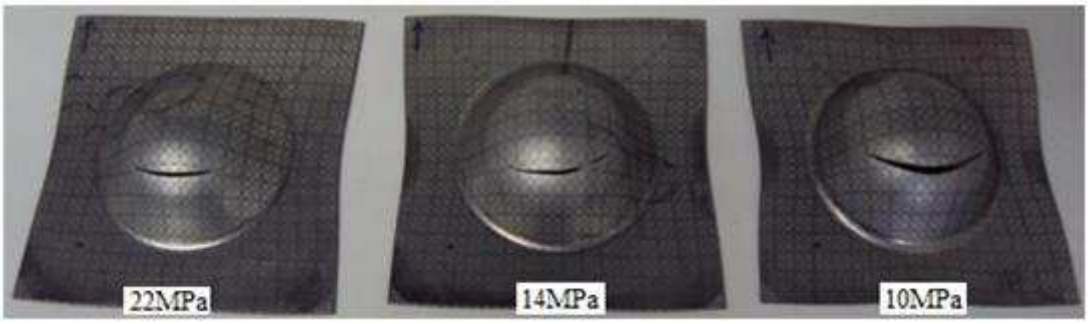

Figure 6. 200x200mm samples stamped with different blank-holder loads.

The fracture occurred far from the pole, due to the lack of efficiency of the lubrication, as the experiment was performed without lubricant, causing an uneven strain of the material, Keeler (2000) and Tigrinho (2008).

3.5 Fracture analysis

In order to verify the type of fracture that occurred in the DP600 steel after tensile and stamping tests, there were performed analysis by SEM (Scanning Electron Microscope), for comparison with other authors.

Anderson (1995) classifies the fracture of metallic materials into four types: alveolar, cleavage, intergranular or striations, see Figs. 7 and 8.

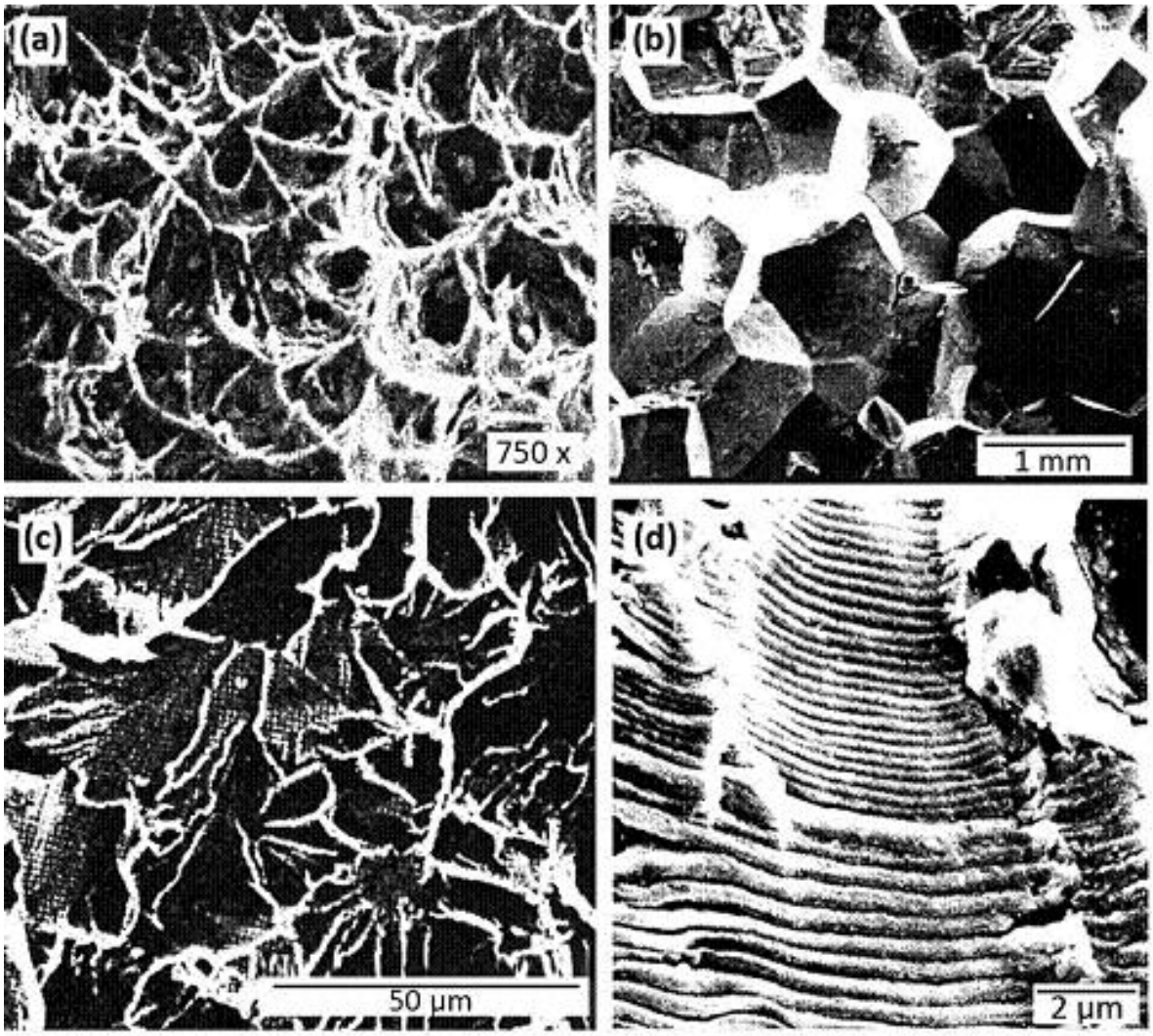

Figure 7. Different fracture types; (a) Alveolar crack; (b) Intergranular crack;
(c) Cleavage crack and (d) Crack striations. (ASM Handbook, 1993)

Anderson (1995) states that all ductile fracture occurs by alveolar mechanism. The cleavage mechanism absorbs so low energy that this fracture mechanism is always fragile. The intergranular mechanism is abnormal in metals, ie, its occurrence is evidence that some embrittlement mechanism occurred during the development or use of the material. The striation mechanism only occurs when the fracture is caused by fatigue.

According to the ASM Handbook (1993), the region characteristic of a ductile fracture, ie, the fibrous region, is always formed by the alveolar mechanism. Figure 8 shows another aspect of this fracture mechanism with noticeable rounded particles inside the alveoli, which originate the alveoli.

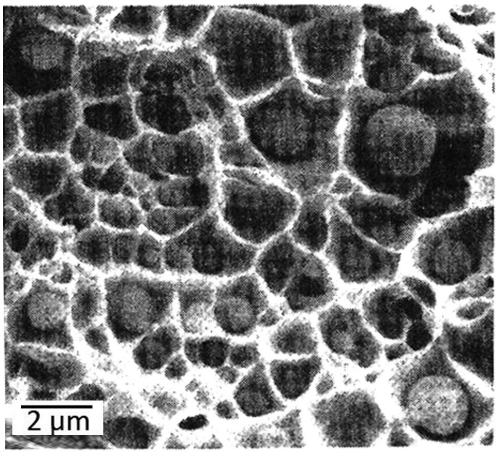

Figure 8. Particles inside the alveoli. (ASM Handbook, 1993)

Figure 9 show the fracture of the steel DP600, after the stamping test with magnifications of 2,500X and 5,000X, respectively. Making a comparison between Figs. 7a and 7c with the Fig. 9, it can be said that the DP600 steel fracture is ductile and of alveolar type due to the ferritic matrix, with regions showing brittle cleavage fracture due to martensitic phase in the steel. Even so, the proportion of ductile fracture is higher due a greater presence of ferrite as compared to the presence of martensite.

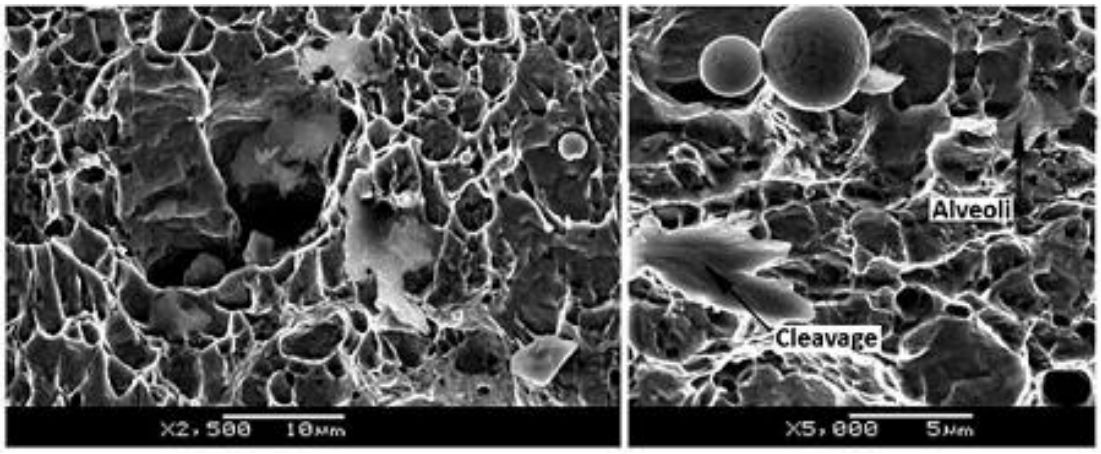

Figure 9. DP600 fracture – 2.500x and 5.000x magnification.

The lower the load applied to the blank-holders, the larger are the quantities of regions presenting cleavage points. Around 22MPa, the fracture is characterized as fully ductile with alveolar type, at 14MPa the first points of cleavage began to appear and around 10MPa the amount of points of cleavage among the alveoli increased in proportion.

4. CONCLUSIONS

Based on experimental and simulation results and comparing them with the information from literature and from the supplier of the raw material, the following conclusions can be made:

a) Chemical analysis: due the outcome of the test performed, it can be said that the DP600 steel presets chemical elements at levels characteristic of a material with good formability, and a close proximity to figures provided by the manufacturer;
b) Metallography: according to the analysis, it is evident the presence of martensite islands into the ferrite matrix, like the photos from the bibliography;
c) Tensile test: mechanical property values were consistent with those obtained by the steel supplier, combining excellent mechanical strength to a good degree of formability;
d) Stamping: by the comparison of the Formability Limit Curves, obtained via Nakazima testing and literature, there is a similarity only at the plain strain. In the other deformation modes, drawing and stretching mainly by the lack of lubrication, the results are quite different;

e) Pressure at the blankhoders: the lower the pressure on the blankhoders, higher the stamping level of the material and there is also an increase in the force required for deformation.
f) Electron microscopy: the DP600 steel showed a higher proportion of ductile fracture of alveolar type due to the ferritic matrix, with areas of brittle fracture by cleavage due to the hard martensite phase.
g) Simulation: Experimental results and simulation of force and displacement of the punch were similar, but the simulation was not able to predict the occurrence of cracks due to limitations in describing the behavior of the material.

5. ACKNOWLEDGEMENTS

Thanks to Usiminas for providing the DP600 steel samples, thereby enabling this research.

6. REFERENCES

Anderson, T. L. *Fracture Mechanics – Fundamentals and Applications* – 2nd Edition, CRC Press, 1995.

Andrade, S. L.; Batista, J. F.; Taiss, J. M.; Rosa, L. K. ULSAB-AVC – O aço no automóvel do futuro: A estratégia da USIMINAS. In: 55º Congresso da Associação Brasileira de Metalurgia e Materiais, 2000, Rio de Janeiro, *Anais*... Rio de Janeiro, Julho 2000.

Andrade, S. L., TAISS, J. M., ROSA, L. K. O aço no automóvel do futuro. In: 57º Congresso da Associação Brasileira de Metalurgia e Materiais, 2002, São Paulo, *Anais*... São Paulo, Julho 2002.

ASM INTERNATIONAL, *Metals Handbook*, vol. 14, 9ª ed., 1993.

Bhadeshia, H. K. D. H. Bainite in Steels. London, *The Institute of Materials*, 2001.

Bleck, W.; Kriangyut, P. O., Microalloying of Cold-Formable Multiphase Steel Grades. *Materials Science Forum*, p. 7-113, 2005.

Chemin Filho, R. A. *Avaliação das deformações de Chapas Finas e Curvas CLC para Diferentes Geometrias de Punções*. 127f. Dissertação (Mestrado em Engenharia Mecânica) – Setor de Tecnologia, Universidade Federal do Paraná, Curitiba, 2004.

De Cooman, B. C. Structure-properties relationship in TRIP steels containing carbide-free bainite. *Current Opinion in Solid State and Materials Science*, 8., p. 285-303, 2004.

Gorni, A. A. Caracterização Topológica da Microestrutura Bifásica, *Revista Escola de Minas*, 49:1, pp. 40-44, Janeiro-Março 1995.

Gorni, A. A. Engenharia Microestrutural das Chapas de Aços de Alta Resistência. In: Conferência Nacional de Conformação de Chapas, 11., Outubro 2008, Porto Alegre. *Anais*... Porto Alegre: Centro Brasileiro de Inovação em Conformação Mecânica, 2008.

Grajcar, A.; Adamczyk, J. Structure and mechanical properties of DP-type and TRIP-type sheets obtained after the thermomechanical processing. *Journal of Materials Processing Technology*, 162-163, p. 267-274, 2005.

Hornbogen, E.; Becker, J.; Stratmann, P. Dual-Phase Gefüge. *Zeitschrift für Metallkunde*, 71(1), p. 27-31, January 1980.

Lajarin, S.F.; Barreto Neto R. da C. and Marcondes P.V.P., "Avaliação numérica do processo de puncionamento de chapa grossa com diferentes formatos de punção", In: VI NATIONAL CONGRESS OF MECHANICAL ENGINEERING, 2010, Campina Grande. 6 CONEM2010.

Keeler, S. P. Understanding Sheet Metal Formability. *Machinery*, 1968.

Keeler, S. P. To Lube or Not to Lube. *Magazine Metal Forming*, p. 68-69, April 2000.

Konieczny, A. *Advanced High Strength Steels – Formability, 2003 Great Designs in Steel***.** American Iron and Steel Institute (February 19, 2003), www.autosteel.org.

Kumar, D. R. Formability analysis of extra-deep drawing steel. *Journal of Materials Processing Technology*, 130 131, p. 31-41, 2002.

Nakazima, K.; Kikuma, T.; Hasuka, K. Study on Formability of Steel Sheets. Yawata Tech. Rep. 1968, p. 141.

Rashid, M. S. GM 980X – Potential Applications and Review. *International Automotive Engineering Congress and Exposition*. S.A.E. Technical Publication n° 770211. Detroit, 12 p., February-March 1977.

Tigrinho, L. M. V. ; Chemin Filho, R. A. ; Santos, R. A. ; Marcondes, P. V. P. *Influência da Lubrificação na Estampagem para Obtenção da Curva CLC*. In: CONGRESSO BRASILEIRO DE ENGENHARIA DE FABRICAÇÃO, 2005, Joinvile. 3 COBEF, 2005.

Tigrinho, L. M. V.; Santos, R. A. dos; Chemin Filho, R. A.; Marcondes, P. V. P. October-December 2008, Experimental Investigation on the Influence of the Lubricant Type in the Punch Stretching of Extra Deep-Drawing Steel. Journal of the Brazilian Society of Mechanical Sciences and Engineering, vol. XXX, issue 4, p. 286-290.

WORLDAUTOSTEEL, *Advanced High Strength Steel (AHSS) Application Guidelines*, Versão 4.1, 2009. Disponível em: www.worldautosteel.org.